18th Australasian Fluid Mechanics Conference
Launceston, Australia
3-7 December 2012

Appropriate Boundary Conditions for a Pressure Driven Boundary Layer

P.J. Richards[1] and S.E. Norris[1]

[1]Department of Mechanical Engineering
University of Auckland, Auckland 1142, New Zealand

Abstract

Velocity and turbulence property profiles are derived for an equilibrium pressure driven atmospheric boundary layer for CFD models using the k-ε turbulence model. It is shown that using these profiles as the inlet conditions on an empty domain results in outlet profiles which are almost identical to the inlet values. It is also shown that using profiles intended for a shear driven situation, but without the driving shear stress, leads to significant changes as the flow relaxes towards matching the free slip boundary condition at the top of the domain.

Introduction

At the first Computational Wind Engineering Conference Richards and Hoxey [1] recommended modelling the atmospheric surface layer as a horizontally-homogeneous turbulent surface layer (HHTSL), which is one with constant properties in directions tangential to the ground and hence the only variation is along the vertical axis. Since the pressure is constant the flow is driven by a shear stress at the upper surface of the layer, and this is constant through the layer, equalling the shear stress at the wall. As noted by Panofsky and Dutton [2] the surface layer is the lowest part of the atmospheric boundary layer, where the shear stress is almost constant and which in moderate to strong winds may extend 100m or more above the ground. Velocity and turbulence property profiles, together with the associated boundary conditions, were proposed for CFD studies using the standard k-ε turbulence model (Launder and Spalding, [3]) and were shown to satisfy horizontal homogeneity provided the various constants satisfied particular relationships. Richards and Hoxey [1] concluded "In order to adequately model the atmospheric surface layer the boundary conditions, turbulence model and associated constants must be consistent with each other". In this regard the boundary conditions included the inlet velocity and turbulence property profiles, the wall functions used at the ground, the driving shear stress and the diffusion of turbulence properties at the top of the domain.

Richards and Hoxey [1] has been cited more than 170 times including about 130 citations in the last 5 years (data obtained from SCOPUS). Many of these citations are from authors who have simply utilised the recommendations, but a number contain related discussions. Bottema [4] has discussed the difference between the level of turbulence kinetic energy (TKE) observed in the atmospheric surface layer and those given by the standard constants of many turbulence models. Blocken et al. [5] focus on wall function problems and the relationship between the wind engineering roughness length and the sand grain roughness commonly used in internal flows. Hargreaves and Wright [6] discuss some of the difficulties with implementing the Richards and Hoxey [1] boundary conditions and note that many computational wind engineers adopt only a subset of these and as a result the turbulence profiles decay along the fetch. They also noted the over production of turbulence kinetic energy in cells near the ground. Recently Yang et al. [7] have proposed alternative k and ε turbulence property profiles but these have been derived by assuming a log-law velocity profile and splitting the turbulence kinetic energy conservation equation into two independent parts, production equal to dissipation and zero diffusion, and solving these. The profiles derived in this manner do not generally satisfy either the ε or momentum equations. Richards and Norris [8] have revisited the analysis of the constant shear stress surface layer and have extended the analysis to include a number of common turbulence models. In addition they have provided an explanation of the excessive production of turbulence kinetic energy often observed in the near wall region.

The Richards and Hoxey [1] recommendations have found their way into various guidelines including those for predicting the pedestrian wind environment by COST (European Cooperation in the field of Scientific and Technical Research) Action C14 "Impact of Wind and Storms on City Life and Built Environment", Working group 2 – CFD Techniques, as reported by Franke [9], and the Architectural Institute of Japan (Tominaga et al. [10]).

Horizontally Homogeneous Turbulent Surface Layer

Richards and Hoxey [1] modeled a HHTSL by proposing velocity and turbulence property profiles, together with the associated boundary conditions, for the standard k-ε turbulence model and showed that these satisfied horizontal homogeneity provided the model constants satisfied particular relationships.

Richards and Norris [8] use an alternative approach to derive the profiles directly from the conservation and equilibrium equations for a HHTSL associated with a particular turbulence model. For example with the standard k-ε model and a rough wall with U=0 at z=z_0 these yield:

$$U = \frac{u_\tau}{\kappa_{k\varepsilon}} \ln\left(\frac{z}{z_0}\right), \quad k = \frac{u_\tau^2}{\sqrt{C_\mu}}, \quad \varepsilon = \frac{u_\tau^3}{\kappa_{k\varepsilon} z} \tag{1}$$

where u_τ is the friction velocity associated with the wall shear stress, which within the surface layer equals the shear stress at all levels

$$\tau = \tau_w = \rho u_\tau^2 \tag{2}$$

The derivation showed that the turbulence model effectively chooses its own value for von Kármán's constant κ, such that the usual k-ε turbulence model constants $C_{\varepsilon 1}$ = 1.44, $C_{\varepsilon 2}$ = 1.92, C_μ = 0.09 and σ_ε = 1.3 give

$$\kappa_{k\varepsilon} = \sqrt{\left(C_{\varepsilon 2} - C_{\varepsilon 1}\right)\ \sigma_\varepsilon \sqrt{C_\mu}} = 0.4237 \tag{3}$$

which is just slightly larger than the commonly accepted value κ = 0.41, which will be used in the remainder of this paper.

The form of equation (1) only differs from that given by Richards and Hoxey [1] in terms of the definition of the height at which the velocity is zero. To implement such profiles the shear stress is imposed at the upper boundary of the domain, a zero flux

condition is set for k, and the flux of ε across the top boundary is prescribed as,

$$\frac{\mu_T}{\sigma_\varepsilon}\frac{d\varepsilon}{dz} = -\frac{\rho u_*^4}{\sigma_\varepsilon z} \tag{4}$$

Hargreaves and Wright [6] note that in their experience "many computational wind engineers adopt only a subset of the Richards and Hoxey boundary conditions (i.e. those at the inlet) and assume that the boundary layer will be maintained up to the point at which the building is located". However they show that this is not the case, even in the absence of obstructions, and that the velocity and turbulence profiles decay along the fetch under these conditions. In their numerical modelling they initially investigate an empty domain, deliberately ignore the shear stress at the top of the domain, "since many practitioners ignore this requirement", but instead decide "that a symmetry condition would suffice" for the demonstration. Without the driving shear stress the problem becomes a pressure driven boundary layer, within which the shear stress varies with height, and while equilibrium profiles may exist these will be different from the constant shear stress case. It is such pressure driven boundary layers that are the subject of the analysis in the next section.

The Equilibrium Pressure Driven Boundary Layer

As noted in the previous section many computational wind engineers will set up a problem by choosing a turbulence model, defining the inlet conditions and will probably define the roughness of the ground plane. However they will leave the top boundary as a default free-slip symmetry boundary. As a result the flow is driven through the domain by a pressure difference between inlet and outlet. In this section we seek to find velocity and turbulence property profiles that will result in an equilibrium boundary layer under such conditions. The turbulence model considered is the standard k-ε model of Launder and Spalding [3] although a similar analysis is possible with most of the standard turbulence models. The solution domain considered, see figure 1, is an empty domain of height H but arbitrary width and length. The pressure is assumed to decrease at a steady rate in the streamwise direction, while being constant across all heights. All other variables are assumed to be independent of both the x and y co-ordinates but may vary with height z above the ground plane.

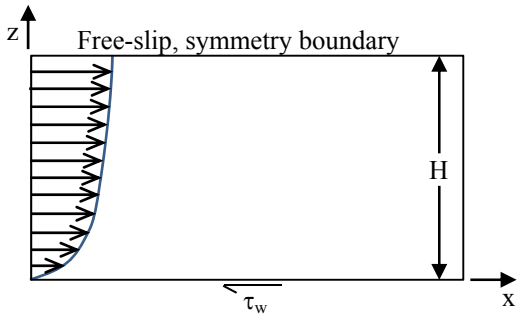

Figure 1. Layout schematic of the solution domain.

In many CFD problems the inlet conditions are defined in terms of the velocity and turbulence property profiles. The computer code is then used to determine such things as the wall shear stress or the pressure differential required to drive the prescribed flow through the domain. In this analysis this order is reversed and it is assumed that the driving pressure gradient is known and the analysis seeks to determine the velocities and turbulence profiles which would match this driving force. While these conditions can be obtained by either running a CFD model with a long fetch or with cyclic boundary conditions, the approach taken here is to analyse the basic equations for this situation.

If the flow is in equilibrium then the forces must be balanced both on the entire domain and on a sub-domain up to height z. As a result

$$\frac{dp}{dx}H = \tau_w = \rho u_\tau^2 \tag{5}$$

and

$$\tau(z) = \tau_w(1 - z/H) \tag{6}$$

where ρ is the fluid density, u_τ the friction velocity based on the wall shear stress τ_w and $\tau(z)$ the variation of shear stress with height.

In this analysis it is assumed that the turbulent shear stress is much larger than the viscous stress and hence

$$\tau(z) = \mu_t \frac{dU}{dz} \tag{7}$$

where μ_t is the eddy viscosity, which with the standard k-ε model is related to the turbulence kinetic energy (k) and its rate of dissipation (ε) by

$$\mu_t = C_\mu \rho \frac{k^2}{\varepsilon} \tag{8}$$

Since the solution sought is for the equilibrium situation the total derivatives of the turbulence properties is zero and so the standard conservation equations are simplified to

$$\rho\frac{Dk}{Dt} = 0 = \mu_t\left(\frac{dU}{dz}\right)^2 - \rho\varepsilon + \frac{d}{dz}\left(\mu_t\frac{dk}{dz}\right) \tag{9}$$

$$\rho\frac{D\varepsilon}{Dt} = 0 = C_{\varepsilon 1}\mu_t\left(\frac{dU}{dz}\right)^2\frac{\varepsilon}{k} - C_{\varepsilon 2}\rho\frac{\varepsilon^2}{k} + \frac{d}{dz}\left(\frac{\mu_t}{\sigma_\varepsilon}\frac{d\varepsilon}{dz}\right) \tag{10}$$

It may be noted that equation (9) could include σ_k, but since the standard value is 1.0 it has been omitted for simplicity.

The velocity derivative in equations (9) and (10) can be replaced by using the relationships in equations (6) and (7) yielding

$$0 = \mu_t\left(\frac{\tau_w(1 - z/H)}{\mu_t}\right)^2 - \rho\varepsilon + \frac{d}{dz}\left(\mu_t\frac{dk}{dz}\right) \tag{11}$$

$$0 = C_{\varepsilon 1}\mu_t\left(\frac{\tau_w(1 - z/H)}{\mu_t}\right)^2\frac{\varepsilon}{k} - C_{\varepsilon 2}\rho\frac{\varepsilon^2}{k} + \frac{d}{dz}\left(\frac{\mu_t}{\sigma_\varepsilon}\frac{d\varepsilon}{dz}\right) \tag{12}$$

In order to obtain a more general result these equations can be transformed into a non-dimensional form by normalising the variables in the following manner

$$z^* = \frac{z}{H},\quad U^* = \frac{U}{u_\tau},\quad k^* = \frac{k}{u_\tau^2},\quad \varepsilon^* = \frac{\varepsilon H}{u_\tau^3},$$
$$\mu_t^* = \frac{\mu_t}{\rho u_\tau H},\quad \tau^* = \frac{\tau}{\rho u_\tau^2} \tag{13}$$

and eliminating the eddy viscosity by using equation (8), which gives

$$0 = \frac{(1 - z^*)^2}{C_\mu}\frac{\varepsilon^*}{k^{*2}} - \varepsilon^* + \frac{d}{dz^*}\left(\frac{C_\mu k^{*2}}{\varepsilon^*}\frac{dk^*}{dz^*}\right) \tag{14}$$

$$0 = C_{\varepsilon 1}\frac{(1 - z^*)^2}{C_\mu}\frac{\varepsilon^{*2}}{k^{*3}} - C_{\varepsilon 2}\frac{\varepsilon^{*2}}{k^*} + \frac{d}{dz^*}\left(\frac{C_\mu k^{*2}}{\sigma_\varepsilon \varepsilon^*}\frac{d\varepsilon^*}{dz^*}\right) \tag{15}$$

This pair of linked equations has been solved using finite-difference approximations. The boundary conditions used are given in table 1 and the resulting profiles plotted in figure 2. At the top of the domain both k^* and ε^* reach their minimum, but both are still finite since the diffusion (last terms in equations (14-15)) is matched by the dissipation (2nd to last terms).

Variable	Near ground, $z^* \to 0$	Top, $z^* = 1$
k^*	$k^* \to \frac{1}{\sqrt{C_\mu}}$	$\frac{dk^*}{dz^*} = 0$
ε^*	$\varepsilon^* = \frac{C_\mu^{0.75} k^{*1.5}}{\kappa z^*}$	$\frac{d\varepsilon^*}{dz^*} = 0$

Table 1. Boundary conditions for the turbulence property equations.

In order to make the results more readily accessible polynomial expressions have been fitted to the computed values. The k^* values are matched to within ±0.3% by

$$k^* = f(z^*) = 0.923 + 3.516(1-z^*)^2 - 1.893(1-z^*)^4 + 0.787(1-z^*)^6 \quad (16)$$

This form has been chosen since it provides a good match while maintaining a zero derivative at $z^* = 1$. It may be noted that at $z^* = 0$, $k^* = 3.333$, as required by the boundary conditions. In later equations $f(z^*)$ is used to represent this polynomial.

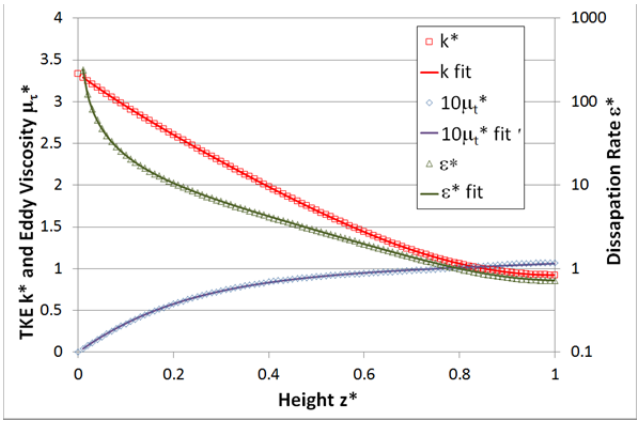

Figure 2. Calculated equilibrium turbulence property profiles. For clarity the eddy viscosity has been multiplied by 10 and ε^* is plotted against a log scale secondary axis. The symbols are the computed values while the lines are the fitted relationships given by equations (16, 19 & 20).

It was found that the dissipation rate could not be readily matched by a similar polynomial and that while the eddy viscosity could be matched, a simpler result could be obtained by first calculating the velocity gradient from

$$\frac{dU^*}{dz^*} = \frac{\tau^*}{\mu_\tau^*} = \frac{1-z^*}{\mu_\tau^*} \quad (17)$$

The resulting data is well matched by the polynomial

$$\frac{dU^*}{dz^*} = g(z^*) = \frac{2.44}{z^*} + 1.7 + 1.29z^* - 8.01z^{*2} + 2.58z^{*3} \quad (18)$$

In fitting the data the limits that $g(1.0) = 0$ and as $z^* \to 0$, $z^* g(z^*) = 1/\kappa = 1/0.41 = 2.44$ were prescribed. An expression for the eddy viscosity may be obtained by substituting this polynomial, $g(z^*)$, into a rearranged equation (17):

$$\mu_\tau^* = \frac{1-z^*}{g(z^*)} \quad (19)$$

and hence the dissipation rate from equation (8) giving

$$\varepsilon^* = \frac{C_\mu f^2(z^*) g(z^*)}{1-z^*} \quad (20)$$

The resulting fits are shown in figure 2. The agreement is not as good as for TKE but the fitted relationships match to within ±3%.

Equation (18) may be integrated to give the velocity profile

$$U^* = 2.44\ln(z^*) + 1.7z^* + 0.645z^{*2} - 2.67z^{*3} + 0.645z^{*4} + \text{constant} \quad (21)$$

The constant is evaluated by using an appropriate velocity boundary condition at the ground. If the simple condition of a rough wall with U=0 at $z=z_0$ and $z_0 \ll H$ is used then the constant can be taken as $-2.44\ln(z_0^*)$. Hence equation (21) becomes

$$U^* = \frac{1}{\kappa}\ln\left(\frac{z^*}{z_0^*}\right) + 1.7z^* + 0.645z^{*2} - 2.67z^{*3} + 0.645z^{*4} \quad (22)$$

This can be transformed back into a dimensional form as

$$U(z) = \frac{u_\tau}{\kappa}\left(\ln\left(\frac{z}{z_0}\right) + 0.698\left(\frac{z}{H}\right) + 0.2645\left(\frac{z}{H}\right)^2 - 1.095\left(\frac{z}{H}\right)^3 + 0.2645\left(\frac{z}{H}\right)^4\right) \quad (23)$$

This is similar in form to the Deaves and Harris [11] model for the complete atmospheric boundary layer used by wind loading codes such as AS/NZS 1170.2 [12]. However the coefficients are quite different.

The corresponding dimensional forms for the turbulence properties are

$$k(z) = u_\tau^2\left(0.923 + 3.516\left(1-\frac{z}{H}\right)^2 - 1.893\left(1-\frac{z}{H}\right)^4 + 0.787\left(1-\frac{z}{H}\right)^6\right) \quad (24)$$

$$\varepsilon(z) = \frac{C_\mu k(z)^2}{u_\tau \kappa z}\left(1 + 1.7\left(\frac{z}{H}\right) + 2.23\left(\frac{z}{H}\right)^2 - 1.06\left(\frac{z}{H}\right)^3\right) \quad (25)$$

Numerical Modelling

To demonstrate the ability of the boundary conditions to represent an equilibrium pressure driven boundary layer, they were prescribed at the inlet of flow through an empty domain. The profiles at the outlet of the domain could then be compared with the inlet values, to see if the inlet values were actually in equilibrium, and also as a test of the ability of the CFD code solver to model such a flow. If the boundary conditions accurately describe the pressure driven flow, then there should be little difference between the values at the inlet and outlet of the domain.

The model problem used was the same as that given by [6], and a schematic of the domain is shown in Figure 3 below. The inlet flow had a reference velocity of 10 m/s at a reference height of 6 m, with a ground roughness of $z_0 = 0.01$ m. The flow was modelled using CFX 14.0 using the standard *k-ε* model. Profiles of the velocity and the turbulence scalars were extracted at the inlet and outlet of the domain and are plotted in Figures 4 and 5, and are labelled *P driven*. For comparison purposes, a calculation was also made using the shear driven flow boundary conditions described in [8] at the inlet, but still using a free slip surface at the high-*z* boundary, and these profiles are labelled *τ driven*.

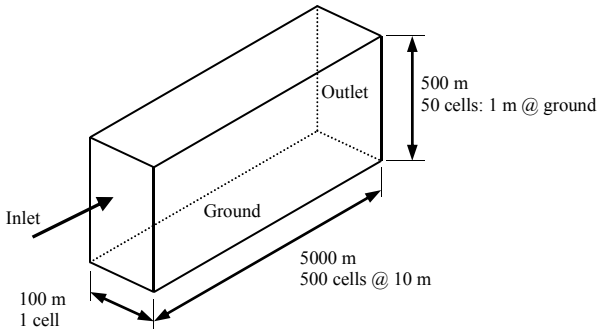

Figure 3. Schematic of the computational domain.

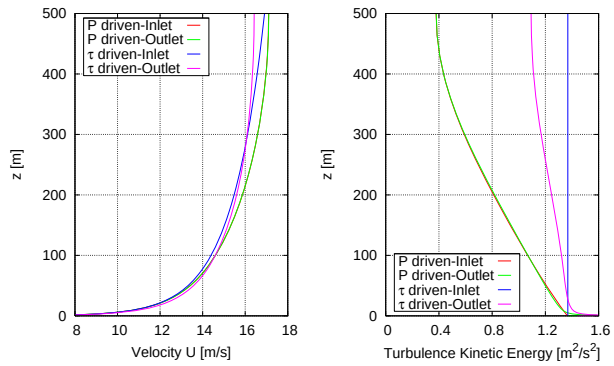

Figure 4. Velocity profiles (left) and turbulence kinetic energy (right) at the inlet and outlet of the computational domain.

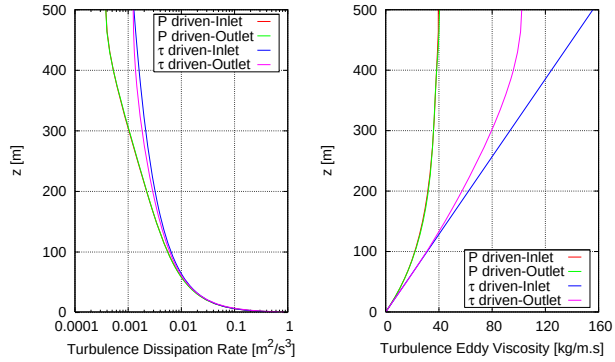

Figure 5. Profiles of turbulence dissipation rate (left) and eddy viscosity (right) at the inlet and outlet of the computational domain.

Examination of Figures 4 and 5 show that there is little difference between the inlet and outlet profiles for the flow calculated using pressure driven inlet conditions, with the two profiles almost overlaying each other for the velocity, turbulence scalars and eddy viscosity. The most notable difference between inlet and outlet conditions is for the profile of the turbulence kinetic energy, where at the outlet the calculated profile exhibits a spike at the near wall node. This is due to the use of cell centred differencing for the calculation of the turbulence production term, as described in [8].

In contrast, the calculation using inlet profiles appropriate for a shear driven flow, but without a shear stress at the top surface, exhibit a large difference between the inlet and outlet profiles. This signifies that the flow is developing in the streamwise direction, with the profiles relaxing to fit the free slip boundary condition at the top of the domain.

Conclusions

CFD calculations of wind engineering flows often inappropriately use inlet boundary conditions derived for a shear driven flow, when the flow being modelled is driven by a pressure gradient through the domain. Boundary conditions have been derived for a pressure driven flow, and have been successfully applied to modelling flow through an empty computational domain.

References

[1] Richards, P.J. & Hoxey, R.P., Appropriate boundary conditions for computational wind engineering models using the k-ε turbulence model. *Journal of Wind Engineering and Industrial Aerodynamics,* 46 & 47, 1993, 145-153.

[2] Panofsky, H.A. & Dutton J.A., *Atmospheric Turbulence*. Wiley-Interscience. 1984.

[3] Launder, B.E. & Spalding, D.B., The numerical computation of turbulent flows. *Computer Methods in Applied Mechanics and Engineering*, 3, 1974, 269-289.

[4] Bottema, M., Turbulence closure model "constants" and the problems of "inactive" atmospheric turbulence. *Journal of Wind Engineering and Industrial Aerodynamics*, 67&68, 1997, 897-908.

[5] Blocken, B., Stathopoulos, T. & Carmeliet, J., CFD simulation of the atmospheric boundary layer: wall function problems. *Atmospheric Environment*, 41, 2007, 238-252.

[6] Hargreaves, D.M. & Wright, N.G., On the use of the k-ε model in commercial CFD software to model the neutral atmospheric boundary layer. *Journal of Wind Engineering and Industrial Aerodynamics*, 95, 2007, 355-369.

[7] Yang, Y., Gu, M., Chen, S. & Jin X., New inflow boundary conditions for modelling the neutral equilibrium atmospheric boundary layer in computational wind engineering. *Journal of Wind Engineering and Industrial Aerodynamics*, 97, 2009, 88-95.

[8] Richards, P.J. & Norris, S.E., 'Appropriate boundary conditions for computational wind engineering models revisited', *Journal of Wind Engineering and Industrial Aerodynamics*, 99, 2011, 257-266.

[9] Franke, J., Recommendations of the COST action C14 on the use of CFD in predicting pedestrian wind environment. *Fourth International symposium on Computational Wind Engineering,* Yokohama, Japan, July 2006.

[10] Tominaga Y., Mochida A., Yoshie, R., Ktaoka H., Nozu T., Yoshikawa M. & Shirasawa T., AIJ guidelines for practical applications of CFD to pedestrian wind environment around buildings. *Journal of Wind Engineering and Industrial Aerodynamics*, 96, 2008, 1749-1761.

[11] Deaves D.M. & Harris R.I., A mathematical model of the structure of strong winds, CIRIA Report 76, Construction Industry Research and Information Association, London, 1978.

[12] AS/NZS 1170.2:2011, Australia/New Zealand Standard, Structural design actions, Part 2: Wind actions, *Standards Australia Limited/Standards New Zealand*, 2011.